Ultrafast electrical charging and discharging of a single InGaAs quantum dot

J. Nannen,[1,a)] T. Kümmell,[1] M. Bartsch,[2] K. Brunner,[3] and G. Bacher[1]
[1]*Werkstoffe der Elektrotechnik und CeNIDE, Universität Duisburg-Essen, Bismarckstraße 81, 47057 Duisburg, Germany*
[2]*Experimentalphysik und CeNIDE, Universität Duisburg-Essen, Lotharstraße 1, 47048 Duisburg, Germany*
[3]*Physikalisches Institut (EP3), Universität Würzburg, Am Hubland, 97074 Würzburg, Germany*

(Received 13 July 2010; accepted 5 October 2010; published online 27 October 2010; publisher error corrected 29 October 2010)

We report on ultrafast control of the charge state of a single InGaAs quantum dot in a charge-tunable p-i-n diode structure. Focused ion beam etching is employed to decrease the capacitance of the device to enable radio frequency operation. A time-resolved photoluminescence technique is demonstrated that allows monitoring the charge state with a time-resolution which is limited only by the radiative lifetime of the charged and neutral exciton, respectively. Experimental data show that the charge state can be manipulated on time scales shorter than the radiative lifetime of approximately 1.4 ns. © *2010 American Institute of Physics*. [doi:10.1063/1.3505358]

Semiconductor quantum dots (QD's) have gained a lot of interest as candidates for possible application in future memory devices[1–4] due to their atomiclike density of states. Especially the possibility to electrically and optically address single quantum dots (SQD's) in semiconductor heterostructures has led to memory device concepts using a single electron or a single hole as the carrier of information. Charge-tunable devices which provide electrical control over the number of electrons in either quantum rings[5] or SQD's[6–9] have been demonstrated several years ago. A single carrier in a QD can either be used in a classical way by considering the charge state of a SQD or for quantum memory devices by using its spin as the information carrier. The reported extremely long spin relaxation time[2,10,11] has triggered different approaches for spin-based memory devices.[2,12,13]

For the applicability of a memory device three different components have to be considered: writing information into the QD, storing it for a certain time, and reading it after storage. Different "classical" memory device concepts have been introduced, which make use of either electrons or holes[14,15] in QD ensembles as well as in SQD's. Extraordinary long storage times have been reported for hole-based memories up to room temperature.[14] While the storage time needs to be sufficiently long, writing and reading the information, in this case equivalent to charging and discharging the SQD, has to be achievable on comparatively short time scales. Hole-based memory devices have been reported to achieve writing times of down to 6 ns.[16] Electrical control over a dark-exciton based memory device via GHz bandwidth electrical pulses has been demonstrated in a charge-tunable SQD device.[17] Controlling the charge state of a SQD by tunneling through a short barrier appears to be a key element for the development of devices operating in the ultrahigh frequency regime.

In this paper we focus on the fast electrical charging and discharging of a SQD with a single electron through a thin tunnel barrier by the application of high speed voltage pulses to a p-i-n diode structure. The charge state of the SQD is probed by time-resolved microphotoluminescence (μ-PL).

The p-i-n diode structure was grown by molecular beam epitaxy (MBE) on a Zn-doped *p*-GaAs (100) substrate ($p=1\times 10^{19}$ cm^{-3}). Following a 50 nm thick layer of undoped GaAs, a 50 nm thick undoped AlGaAs blocking layer was deposited. After this a layer of 160 nm undoped GaAs was grown, on top of which the self-assembled QD's were formed by depositing 1.7 ML InAs. The QD layer is followed by a 20 nm thick undoped GaAs layer. The MBE-grown sequence is completed by a 200 nm thick heavily n-doped GaAs layer ($n=3\times 10^{18}$ cm^{-3}). The electrical contact consists of a 60 nm thick layer of Cr capped by a 10 nm thick Au layer. Electrical connections were achieved by defining 200 nm thick Au bond pads with an area of 100×110 μm^2. Nanoapertures with a diameter down to $\sim$300 nm were defined in the metal layers in order to optically address SQD's. μ-PL measurements were performed under constant wave (cw) and pulsed laser excitation at 1.94 eV in a helium flow cryostat at a temperature of $T=4.3$ K. The cryostat was equipped with a high speed semi-rigid coaxial cable in order to ensure ultra high frequency operation.

Figure 1(a) schematically shows a section of the conduction band (CB) and the valence band (VB) edges of our p-i-n diode structure in real space. By applying an external voltage, the QD energy level can be tuned with respect to the Fermi level (dashed line) so that the charge state of the QD can be controlled. The PL spectrum of a SQD under dc biasing is shown as a contour plot in Fig. 1(b). As previously shown by other groups[5–8] the two marked lines can be assigned to the neutral exciton (X^0) and charged exciton (X^-) emission, respectively, separated by an energy splitting of $\sim$7 meV due to Coulomb interaction. Under reverse biasing an almost abrupt change between the two emission lines can be observed at an external voltage of -0.9 V, which is attributed to the rather high probability for electrons to tunnel through the short triangular barrier of 20 nm.[8] The intensities of the two emission lines extracted from the PL spectra are displayed in Fig. 1(c). Note that the intensity of the X^0 emission is significantly reduced as compared to the X^- emission due to the higher electric field in the sample and an enhanced

[a)]Electronic mail: joerg.nannen@uni-due.de.

 © 2010 American Institute of Physics

Downloaded 30 Oct 2010 to 134.91.4.52. Redistribution subject to AIP license or copyright; see http://apl.aip.org/about/rights_and_permissions

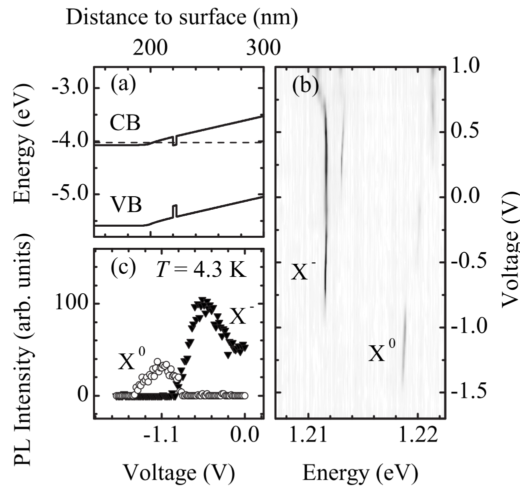

FIG. 1. (a) Schematic section of the band structure of the device, showing the CB and the VB edges. The Fermi level is shown as a dashed line. (b) Contour plot showing the bias voltage-dependent PL spectra. (c) Emission intensities of the charged exciton (X^-) and the neutral exciton (X^0) versus bias voltage.

probability of the photoexcited electron to tunnel out of the SQD under reverse bias condition.

Calculating the tunneling escape rate for electrons from the QD's under study according to Ref. 18 with typical values for a barrier height of ~100 meV and an electric field of ~50–100 kV/cm under reverse biasing leads to estimated tunneling times in the range of 100 ps to a few nanoseconds, which makes subnanosecond control of the charge state of a SQD via short voltage pulses feasible.

Ultrafast performance of the p-i-n device was achieved by choosing the design of the electrical and the optical access as follows. The bond pads were defined in close proximity next to an array of nanoapertures. Around this area approximately 2 μm deep and 1 μm wide trenches were introduced. A scanning electron microscopy image of this design can be seen in the inset of Fig. 2(a). The trenches were etched in a focused ion beam system with Ga ions in combination with injected iodine gas to increase the etch rate. An area of approximately 190×115 μm^2 was thus separated from the remaining sample surface in order to decrease the "parallel plate" capacitance formed by the metal shadow mask and the sample's back contact.[17,19] The current-voltage characteristics of this separated part of the sample at room temperature is shown in Fig. 2(a) and shows

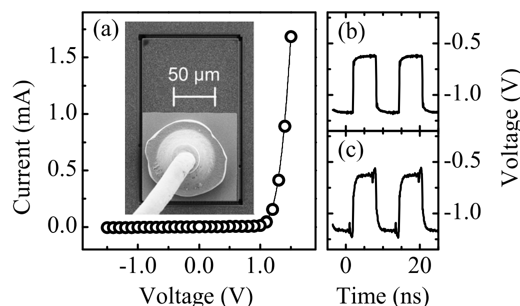

FIG. 2. (a) Voltage-current characteristics of the sample at room temperature. A scanning electron microscopy image of the sample design is shown in the inset. (b) Voltage output from the PPG. (c) Sum of the voltage output from the PPG and reflections from the sample including electrical connections measured on an oscilloscope.

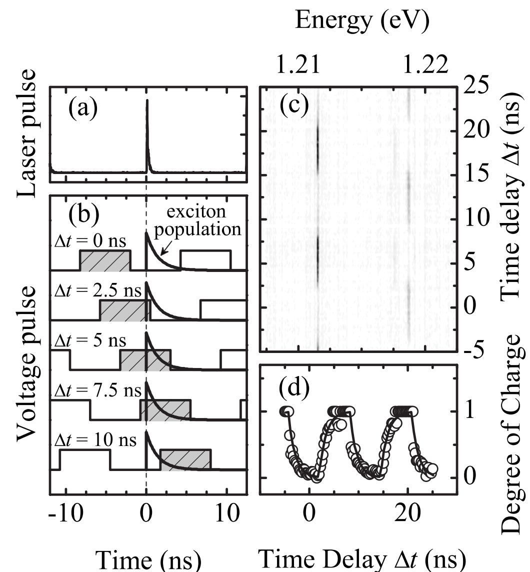

FIG. 3. [(a) and (b)] Schematics of the applied measurement technique: (a) the laser pulse, (b) the time-delayed voltage output from the PPG for five different values of the time-delay Δt. The exciton population after laser excitation is shown as a solid line. (c) Contour plot of the PL spectra as a function of Δt. (d) Degree of charge versus Δt. Open circles: experimental results, solid line: calculation.

the typical behavior of a p-n junction with negligible current in reverse direction.

Square voltage pulses with a duty cycle of 50% and a repetition frequency of 80 MHz were applied to the sample via a 3.35 GHz pulse pattern generator (PPG, 10:90 transition time <100 ps). The voltage levels were set to $V_{high}=-0.6$ V and $V_{low}=-1.2$ V, i.e., to the voltage levels with the most intense emission of the X^- and the X^0 state, respectively, observed in the dc measurements shown in Fig. 1(c). The voltage pulse pattern recorded with a 12 GHz oscilloscope is shown in Fig. 2(b). The observed transition times are proved to be less than 100 ps. In order to get an impression of the radio frequency capability of the system, the sample and the oscilloscope both were connected to the PPG via an electrical power splitter. In this case the acquired signal measured with the oscilloscope is the sum of the part of the pulse which is transferred to the oscilloscope and possible reflections of the electric signal from the sample and electrical connections within the cryostat. The measured signal is shown in Fig. 2(c). A partly reflected signal with an amplitude of ~80 mV can be seen at both edges of the voltage pulse. Also the rising and falling times of the measured signal are slightly increased as compared to the signal shown in Fig. 2(b). However, the lack of considerable reflections as well as the measured transition times of ~300 ps of the measured signal leads to the conclusion that the sample can be operated with voltage pulses with subnanosecond rise and fall times.

Schematics of our time-resolved μ-PL measurement technique are shown in Figs. 3(a) and 3(b): The trigger output of the PPG was connected to the synchronization input of the laser system, so that a laser pulse with a duration of ~200 ps full width at half maximum was triggered with a repetition frequency of 80 MHz. This laser pulse is used to probe the charge state of the SQD by generating an electron-hole pair in the charged or uncharged dot at a well-defined point in time. The voltage output of the PPG could be de-

Downloaded 30 Oct 2010 to 134.91.4.52. Redistribution subject to AIP license or copyright; see http://apl.aip.org/about/rights_and_permissions

layed with respect to the trigger signal—and thus the laser generation of the electron-hole pair—by an adjustable value Δt with an accuracy of ~ 20 ps.

The time delay Δt was varied from -5 to 25 ns in steps of 250 ps. The recorded PL spectra are shown as a function of the respective time-delay Δt in the contour plot in Fig. 3(c). The fingerprint of the applied voltage pulses can be seen in the alternating emission of the X^0 and the X^- state. Switching between the X^0 and X^- emission due to the applied voltage pulses is clearly visible to occur within the nanosecond time regime.

Here, it has to be considered that the ultimate switching time between the X^0 and X^- emission is limited by the radiative lifetime, even if the charging and the discharging time of the SQD is significantly faster. This aspect can be seen in the schematics shown in Figs. 3(a) and 3(b). In Fig. 3(a), the temporal profile of the laser pulse is shown, while in Fig. 3(b), the resulting transient exciton population is depicted together with the sequence of the electrical pulse, time delayed by Δt with respect to the laser pulse. Depending on Δt, the laser excites the QD that is either charged (high voltage level) by an additional electron or not (low voltage level). In case of instantaneous recombination of the electron-hole pair, the recorded PL would only render the X^- or the X^0 state. But in case of a finite exciton lifetime, the charge state of the QD might change prior to recombination, as shown for example in the bottommost picture in Fig. 3(b). Here, the laser excites an electron-hole pair in the uncharged dot. Nevertheless, a considerable number of electron-hole pairs stays in the excited state until the quantum dot gets charged with an additional electron by the following voltage pulse. So there will be a distinct contribution to the X^- signal, dependent on the time delay Δt, despite the quantum dot was uncharged during excitation.

We measured the radiative lifetime on a reference sample from the same wafer. The transient PL after pulsed laser excitation was recorded at the peak energy of the inhomogeneously broadened emission spectrum of the QD ensemble at approximately 1.33 eV and a recombination time of 1.4 ns was found (data not shown).

For further evaluation of the charging and discharging times we define the degree of charge as the intensity of the charged exciton emission divided by the sum of the charged and uncharged exciton emission intensities: DoC $=I(X^-)/[I(X^-)+I(X^0)]$. The intensities are each normalized by their respective maximum value in order to pay respect to the different electric field dependent emission intensities. The degree of charge is shown in Fig. 3(d).

We performed a numerical model simulation for the transient change in the degree of charge. In a first approximation we used infinitively small rise and fall times of the applied bias voltage as well as infinitively small tunneling times for our calculations. The only parameter in this model is the radiative lifetime, which was chosen as 1.4 ns according to previous experimental results. The degree of charge calculated with this model is shown as a solid line in Fig. 3(d). Our experimental findings are very well reproduced by this simple calculation, which shows that indeed the radiative lifetime is the limiting factor for this measurement technique. From these results we conclude that the electron tunneling process into and out of the SQD happens on time scales faster than the radiative lifetime, i.e., faster than 1.4 ns. Considering the fact that the recombination time of an electron-hole pair in a SQD under reverse bias conditions is expected to be reduced due to tunneling and, in addition, the overall decay characteristics changes from a mono-exponential decay for the X^- state to a nonexponential decay for the X^0 emission due to the influence of dark exciton states (Ref. 20), an asymmetry of the temporal switching between the X^0 and X^- emission might be expected, but has up to now not been observed due to the achievable precision of our measurements.

In conclusion we have demonstrated a time-resolved measurement technique with a resolution only limited by the electron-hole recombination time which allows for the monitoring of the ultrafast charging and discharging behavior of a single InGaAs quantum dot in a charge-tunable device. Our measurements show that the charging of a SQD with an electron from the n-doped region as well as the discharging of the SQD can be controlled on a time scale only limited by our experimental resolution of approximately 1.4 ns.

The authors would like to thank J. Wenisch, N. Stracke, H. Watzel, and D. Iavarone for sample preparation and W. Quitsch C. Blumberg and O. Pfingsten for experimental assistance. Financial support from the DFG via the SFB 491 is gratefully acknowledged.

[1] *Single Semiconductor Quantum Dots*, edited by P. Michler (Springer, New York, 2009).
[2] M. Kroutvar, Y. Ducommun, D. Heiss, M. Bichler, D. Schuh, G. Abstreiter, and J. J. Finley, Nature (London) **432**, 81 (2004).
[3] G. Yusa and H. Sakaki, Appl. Phys. Lett. **70**, 345 (1997).
[4] C. Balocco, A. M. Song, and M. Missous, Appl. Phys. Lett. **85**, 5911 (2004).
[5] R. J. Warburton, C. Schäflein, D. Haft, F. Bickel, A. Lorke, K. Karrai, J. M. Garcia, W. Schoenfeld, and P. M. Petroff, Nature (London) **405**, 926 (2000).
[6] F. Findeis, M. Baier, A. Zrenner, M. Bichler, G. Abstreiter, U. Hohenester, and E. Molinari, Phys. Rev. B **63**, 121309(R) (2001).
[7] J. J. Finley, P. W. Fry, A. D. Ashmore, A. Lemaître, A. I. Tartakovskii, R. Oulton, D. J. Mowbray, M. S. Skolnick, M. Hopkinson, P. D. Buckle, P. A. Maksym, Phys. Rev. B **63**, 161305(R) (2001).
[8] M. Baier, F. Findeis, A. Zrenner, M. Bichler, and G. Abstreiter, Phys. Rev. B **64**, 195326 (2001).
[9] J. Seufert, M. Rambach, G. Bacher, A. Forchel, T. Passow, and D. Hommel, Appl. Phys. Lett. **82**, 3946 (2003).
[10] J. M. Elzerman, R. Hanson, L. H. Willems van Beveren, B. Witkamp, L. M. K. Vandersypen, and L. P. Kouwenhoven, Nature (London) **430**, 431 (2004).
[11] M. Scheibner, T. A. Kennedy, L. Worschech, A. Forchel, G. Bacher, T. Slobodskyy, G. Schmidt, and L. W. Molenkamp, Phys. Rev. B **73**, 081308(R) (2006).
[12] D. Heiss, V. Jovanov, M. Bichler, G. Abstreiter, and J. J. Finley, Phys. Rev. B **77**, 235442 (2008).
[13] M. Ghali, T. Kümmell, J. Wenisch, K. Brunner, and G. Bacher, Appl. Phys. Lett. **93**, 073107 (2008).
[14] A. Marent, M. Geller, A. Schliwa, D. Feise, K. Pötschke, D. Bimberg, N. Akçay, and N. Öncan, Appl. Phys. Lett. **91**, 242109 (2007).
[15] A. Marent, T. Nowozin, J. Gelze, F. Luckert, and D. Bimberg, Appl. Phys. Lett. **95**, 242114 (2009).
[16] M. Geller, A. Marent, T. Nowozin, D. Bimberg, N. Akçay, and N. Öncan, Appl. Phys. Lett. **92**, 092108 (2008).
[17] J. McFarlane, P. A. Dalgarno, B. D. Gerardot, R. H. Hadfield, R. J. Warburton, K. Karrai, A. Badolato, and P. M. Petroff, Appl. Phys. Lett. **94**, 093113 (2009).
[18] E. N. Korol, Sov. Phys. Solid State **19**, 1327 (1977).
[19] V. G. Truong, P.-H. Binh, P. Renucci, M. Tran, Y. Lu, H. Jaffrès, J.-M. George, C. Deranlot, A. Lemaître, T. Amand, and X. Marie, Appl. Phys. Lett. **94**, 141109 (2009).
[20] J. M. Smith, P. A. Dalgarno, R. J. Warburton, A. O. Govorov, K. Karrai, B. D. Gerardot, and P. M. Petroff, Phys. Rev. Lett. **94**, 197402 (2005).

Downloaded 30 Oct 2010 to 134.91.4.52. Redistribution subject to AIP license or copyright; see http://apl.aip.org/about/rights_and_permissions